


Impact of Andrographolide and Melatonin Combinatorial Drug Therapy on Metastatic Colon Cancer Cells and Organoids

Clinical Medicine Insights: Oncology
Volume 15: 1–9
© The Author(s) 2021
Article reuse guidelines:
sagepub.com/journals-permissions
DOI: 10.1177/11795549211012672



Neha Sharda¹, Tamaki Ikuse^{1,2}, Elizabeth Hill¹, Sonia Garcia¹, Steven J Czinn¹, Andrea Bafford³, Thomas G Blanchard¹ and Aditi Banerjee¹ 

¹Department of Pediatrics, University of Maryland School of Medicine, Baltimore, MD, USA.

²Department of Pediatric and Adolescent Medicine, Juntendo University Graduate School of Medicine, Tokyo, Japan. ³Department of Surgery, University of Maryland School of Medicine, Baltimore, MD, USA.

ABSTRACT

BACKGROUND: The death rate (the number of deaths per 100 000 people per year) of colorectal cancer (CRC) has been dropping since 1980 due to increased screening, lifestyle-related risk factors, and improved treatment options; however, CRC is the third leading cause of cancer-related deaths in men and women in the United States. Therefore, successful therapy for CRC is an unmet clinical need. This study aimed to investigate the impacts of andrographolide (AGP) and melatonin (MLT) on CRC and the underlying mechanism.

METHODS: To investigate AGP and MLT anticancer effects, a series of metastatic colon cancer cell lines (T84, Colo 205, HT-29, and DLD-1) were selected. In addition, a metastatic patient-derived organoid model (PDOD) was used to monitor the anticancer effects of AGP and MLT. A series of bioassays including 3D organoid cell culture, MTT, colony formation, western blotting, immunofluorescence, and quantitative polymerase chain reaction (qPCR) were performed.

RESULTS: The dual therapy significantly promotes CRC cell death, as compared with the normal cells. It also limits CRC colony formation and disrupts the PDOD membrane integrity along with decreased Ki-67 expression. A significantly higher cleaved caspase-3 and the endoplasmic reticulum (ER) stress proteins, IRE-1 and ATF-6 expression, by 48 hours were found. This combinatorial treatment increased reactive oxygen species (ROS) levels. Apoptosis signaling molecules BAX, XBP-1, and CHOP were significantly increased as determined by qPCR.

CONCLUSIONS: These findings indicated that AGP and MLT associated ER stress-mediated apoptotic metastatic colorectal cancer (mCRC) cell death through the IRE-1/XBP-1/CHOP signaling pathway. This novel combination could be a potential therapeutic strategy for mCRC cells.

KEYWORDS: Andrographolide, melatonin, metastatic colon cancer, endoplasmic reticulum stress, reactive oxygen species, patient-derived organoids

RECEIVED: December 8, 2020. **ACCEPTED:** March 29, 2021.

TYPE: Original Research Article

FUNDING: The author(s) received no financial support for the research, authorship, and/or publication of this article.

DECLARATION OF CONFLICTING INTERESTS: The author(s) declared the following potential conflicts of interest with respect to the research, authorship, and/or publication of

this article: This study has been the subject of a patent application by T.G.B., S.J.C., and A.B. of the University of Maryland School of Medicine. The current status of the application is pending.

CORRESPONDING AUTHOR: Aditi Banerjee, Department of Pediatrics, University of Maryland School of Medicine, Bressler Research Building, 13-043, 655 W. Baltimore Street, Baltimore, MD 21201, USA. Email: aditi.banerjee@som.umaryland.edu

Introduction

The American Cancer Society (ACS) estimates that, in 2020 alone, there will be 104 610 new diagnoses of colon cancer in the United States. Most colorectal cancers (CRCs) occur in adults aged 50 and older, and 17 930 (12%) of cases are diagnosed in individuals younger than age 50, the equivalent of 49 new cases per day.¹ Chemotherapy, targeted therapy, and immunotherapy are the current treatment options for CRC, though each strategy has its own limitations.^{2–4} Therefore, targeting metastatic colorectal cancer (mCRC) cells via molecular targets remain important in colon cancer therapy.

Combination therapy, a treatment modality which combines 2 or more therapeutic agents, is a cornerstone of cancer

therapy.^{5,6} Moreover, this therapy is a promising strategy for synergistic anticancer treatment. It has different mechanisms of action that could reduce the dose of each agent, thus may reduce the individual drug-related toxicity.⁶ The studies were carried out if 2 combinatorial drugs have an impact of metastatic colon cancer cells and stage III patient-derived organoids. Earlier studies have demonstrated that the plant metabolite andrographolide (AGP) induces CRC cell death due to apoptosis and is associated with the activation of IRE-1, an endoplasmic reticulum (ER) stress marker.⁷ Additional studies showed that AGP induces apoptotic cell death through the induction of reactive oxygen species (ROS), which eventually play a role in down-regulating cell cycle



Creative Commons Non Commercial CC BY-NC: This article is distributed under the terms of the Creative Commons Attribution-NonCommercial 4.0 License (<https://creativecommons.org/licenses/by-nc/4.0/>) which permits non-commercial use, reproduction and distribution of the work without further permission provided the original work is attributed as specified on the SAGE and Open Access pages (<https://us.sagepub.com/en-us/nam/open-access-at-sage>).

progression and cell survival pathways.⁸ AGP also induces cell death through the inhibition of angiogenic signaling, which is inversely related to the tumor suppressor gene expression, RASSF1A.⁹ Co-treatment of AGP with other substances suggests its potential in combination therapies. In the context of cancer, AGP can diminish resistance to 5-fluorouracil (5-FU), a first-line chemotherapeutic agent for patients with CRC.^{10,11}

Recent studies have also shown that melatonin (MLT) has antimetastatic properties by modulating cell–cell and cell–matrix interactions, remodeling the extracellular matrix, and suppressing angiogenesis.^{12–14} In addition, extensive experimental data demonstrates that this chronobiotic agent exerts oncostatic effects throughout all stages of tumor growth, from initial cell transformation to mitigation of malignant progression and metastasis; additionally, MLT alleviates the side effects and improves the welfare of radio/chemotherapy-treated patients.¹⁵ Moreover, it inhibits CRC proliferation by increasing ROS and inducing apoptosis, autophagy, and senescence.¹⁶ In addition, MLT also causes drug-resistant CRC cell death and inhibits CRC-colospheroids when it is co-administered with 5-FU.¹⁷ In this study, we tested the potential of AGP to inhibit CRC cell growth with reduced concentration compared with prior studies when combined with the safe, anticancer compound MLT. We demonstrate this dual compound has an impact on metastatic CRC cells (T84, Colo 205, HCT-15, HT-29, and DLD-1) and requires a concentration 3 times less than in previous studies. Moreover, these combinatorial therapies exert a little impact on normal cells.

Methods

Ethics statement

All de-identified metastatic colon cancer tissues were received from the surgery of colon cancer patients with the approval of the University of Maryland Institutional Review Board (HP-00066889-4). Written consent was obtained from all patients from whom discarded tissue was collected which included permission to publish results. A small piece of each tumor tissue was frozen for subsequent analysis and remaining tissue was processed for organoid cultures.

Generation and propagation of patient-derived organoid cell cultures (PDOD)

Organoid cells were generated from stage 3 metastatic cancer tissue and cultured as previously described.^{9,18,19} The cultures were passaged when the aggregates reached a diameter of approximately 800 μm . Organoids were treated with 15 μM AGP, 0.5 mM MLT, or both for 48 hours. Treated and untreated organoids were subjected to morphological analysis and immunofluorescence for Ki67 expression.

Cell culture and drug treatment

T84 and Colo 205 colon cancer cell lines were cultured as previously published.^{7–9,19} HT-29 and DLD-1 were grown in RPMI-1640 nutrient media in a humidified incubator at 37°C with 5% CO₂. All media were supplemented with a 1 \times solution of antimicrobial reagents (10 000 U/mL penicillin, 10 000 streptomycin, and 25 $\mu\text{g}/\text{mL}$ amphotericin B), 1 \times glutamine, and 10% fetal bovine serum (FBS). Mouse normal epithelial cells (GSM06) and prostate epithelial cells (RWPE1) cells were grown and cultured as previously described.¹⁹ When cell was grown 80% confluent, media was replaced with media containing 2% FBS with AGP (Sigma Aldrich, St. Louis, MO) and MLT (a kind gift from Professor Russel J. Reiter) with indicated dose and time point. Stock AGP (100 mM) and MLT (1 M) were prepared in dimethyl sulfoxide (DMSO) and control wells received DMSO at a final concentration of 0.01%.

Cytotoxicity assay

Cytotoxicity assay in the presence or absence of AGP or MLT was assessed using the MTT assay as previously described.⁷

Clonogenic assay

HT-29 and DLD-1 cells were seeded in 6-well plates (approximately 50 000/well). The clonogenic assay was performed as previously described.⁷

Quantitative real-time polymerase chain reaction

Gene expression was evaluated as previously described.⁷ Primer sequences are listed in Supplementary Table 1. Relative gene expression changes were calculated using the 2- $\Delta\Delta\text{CT}$ method and expression normalization was accomplished using the housekeeping gene, GAPDH (glyceraldehyde-3-phosphate dehydrogenase).

Immunoblotting

Immunoblotting was performed as previously described.²⁰ The primary antibodies used were against Cleaved caspase-3 (#MAB835) from R&D Systems, Caspase 3 (#9662), IRE-1(#3294) from Cell Signaling, Cyclin B1 (GNS1, #sc-245), p-PERK (#sc-32577), PRX (A-6) (#sc-137150P), TRX (#sc-271281) from Santa Cruz Biotechnology, ATF-6 (#MA5-16172) from Thermo Fisher Scientific, melatonin receptor 1B or MT2 (#NLS9320 from Novus Biologicals), and GAPDH (G8795) from Sigma Aldrich. Blots were incubated with horseradish peroxidase (HRP)-conjugated secondary antibodies followed by enhanced chemiluminescence (ECL) detection. All secondary antibodies were purchased from KPL, Gaithersburg, MD. Images were captured using a Syngene G

Box digital imager (Frederick, MD, USA) and results were quantified by densitometry as previously described.¹⁹

Immunofluorescence

Patient-derived organoids were grown in 1:1 mixture of Matrigel and advanced Dulbecco's Modified Eagle's medium (DMEM):F12 (Life Technologies) supplemented with 1× penicillin/streptomycin, 1× glutamine, 1× N2, 1× B27, 1 mM *N*-acetyl-L-cysteine, 20 ng/mL fibroblast growth factor, and 50 ng/mL epidermal growth factor at 37°C on a 4-chambered glass slide. Fully grown organoids were treated with or without AGP and MLT for 48 hours. Whole mount staining was carried out as previously described^{9,21} with slight modifications. After desired time of treatment, organoids were washed 3 times with 1× phosphate-buffered saline (PBS) and fixed with 4% paraformaldehyde at room temperature for 30 minutes, permeabilized with 0.2% Triton X-100 for 20 minutes, blocked with 2.5% horse serum (Vector; S-2012) and incubated with 1:40 dilution of Ki-67 (M-19) (#sc-7846) at 4°C for overnight. After incubation, organoids were washed 3 times with PBS (10 min/wash) and incubated with Alexa Flour 488 labeled donkey anti-goat IgG (H + L) (1:200) (ab 150129).

Fluorescence microscopy and image acquisition

Fluorescence microscopy and colony counting were performed using an inverted fluorescence microscope (Olympus IX-71, Pennsylvania, USA). Images for patient-derived organoids (PDOD) were taken at 400× magnification. Fluorescence intensity was quantified using ImageJ software version 1.39 (NIH). RGB composite images from control and treated groups were created using Axion Vision rel, 4.6 and analyzed. Images from 5 different fields were used for statistical analysis as previously described.^{8,9,21}

Statistical analysis

Statistical analysis was performed with Graph Pad Prism for Macintosh 5.0c (Graph Pad Software Inc., San Diego, CA). The mean SE was calculated by 1-way analysis of variance (ANOVA). Significance between groups was analyzed using the post hoc Tukey test and Bonferroni test. A $P < .05$ was considered statistically significant.

Results

Co-treatment with AGP and MLT inhibits cell viability

Previous studies have demonstrated that the IC₅₀ value of AGP for T84 and Colo 205 is 45 μM,⁷ whereas IC₅₀ value of MLT for CRC ranges from 1 to 2.5 mM.^{22,23} To reduce the AGP

concentration, T84, Colo 205, HT-29, and DLD-1 cells were co-treated with AGP (0-150 μM) and MLT (0.5 mM) for 24, 48, and 72 hours to assess the effect on cell proliferation. MTT assays revealed co-treatment significantly reduced cell viability in a time- and dose-dependent manner (Figure 1A to D). The IC₅₀ was determined to be 15 μM for AGP and 0.5 mM for MLT at 48 hours. This concentration was used for subsequent assays. Additional experiments were performed to determine the efficacy of this co-treatment on normal cells such as gastric surface mucous cell lines from transgenic mice GSM06 and normal prostate epithelial cells (RWPE-1). Co-treatment of normal epithelial cells with the same concentration of AGP and MLT had little effect on cell numbers (Figure 1E and F). These data suggest that AGP and MLT co-treatment selectively inhibits CRC cells but not normal cells. The inhibitory properties of AGP and MLT on HT-29 and DLD-1 cells were also determined in a clonogenic assay and direct enumeration of stained colonies (Figure 2). Co-treatment of cells for 48 hours resulted in significantly fewer colonies compared with the untreated cells. Co-treatment significantly decreased the number of colonies ($P < .001$) by 48 hours.

Co-treatment with AGP and MLT induces apoptosis and apoptosis signaling is dependent on ER stress

Earlier studies showed that AGP, at a concentration of 45 μM, causes apoptotic CRC cell death due to the unfolded protein response (UPR)-mediated ER stress pathway.⁷⁻⁹ To verify the function of a lower concentration of AGP on CRC cells, T84 and Colo 205 cells were co-treated with AGP and MLT as indicated. As shown in Figure 3A and B, co-treatment significantly increased the 17 kDa cleaved Caspase 3 levels ($P < .001$) as compared with the control and treatment with either AGP or MLT alone. The ratio of cleaved caspase 3 and total caspase 3 also significantly increased (Figure 3C; $P < .001$). In addition, co-treatment significantly upregulated pro-apoptotic BAX mRNA expression (Figure 3D; $P < .001$), but not mRNA of Bcl-2 (Figure 3E, T84). To verify the apoptotic induction with co-treatment of AGP and MLT is due to the UPR, T84 and Colo 205 mRNA levels were monitored for UPR signaling pathway initiators IRE-1, ATF-6, and PERK. Co-treatment resulted in a significant increase in IRE-1 and ATF-6 mRNA expression (~4.5-6-fold, $P < .001$) at 48 hours (Figure 4A and B). Consistent with IRE-1 activation, an increase in XBP-1 mRNA expression of over 3.5-fold for T84 and 1.5-fold for Colo 205 was observed at 48 hours (Figure 4C; $P < .001$ and $P < .05$). Expression of CHOP, which can be activated by XBP-1, was also significantly increased (Figure 4D; $P < .05$ for T84 and $P < .01$ for Colo 205). An additional experiment was performed to monitor the ER stress protein level (IRE-1, p-PERK, and ATF-6) by western blot. ER stress protein analysis revealed increases only in IRE-1 in T84 and Colo 205 co-treated groups

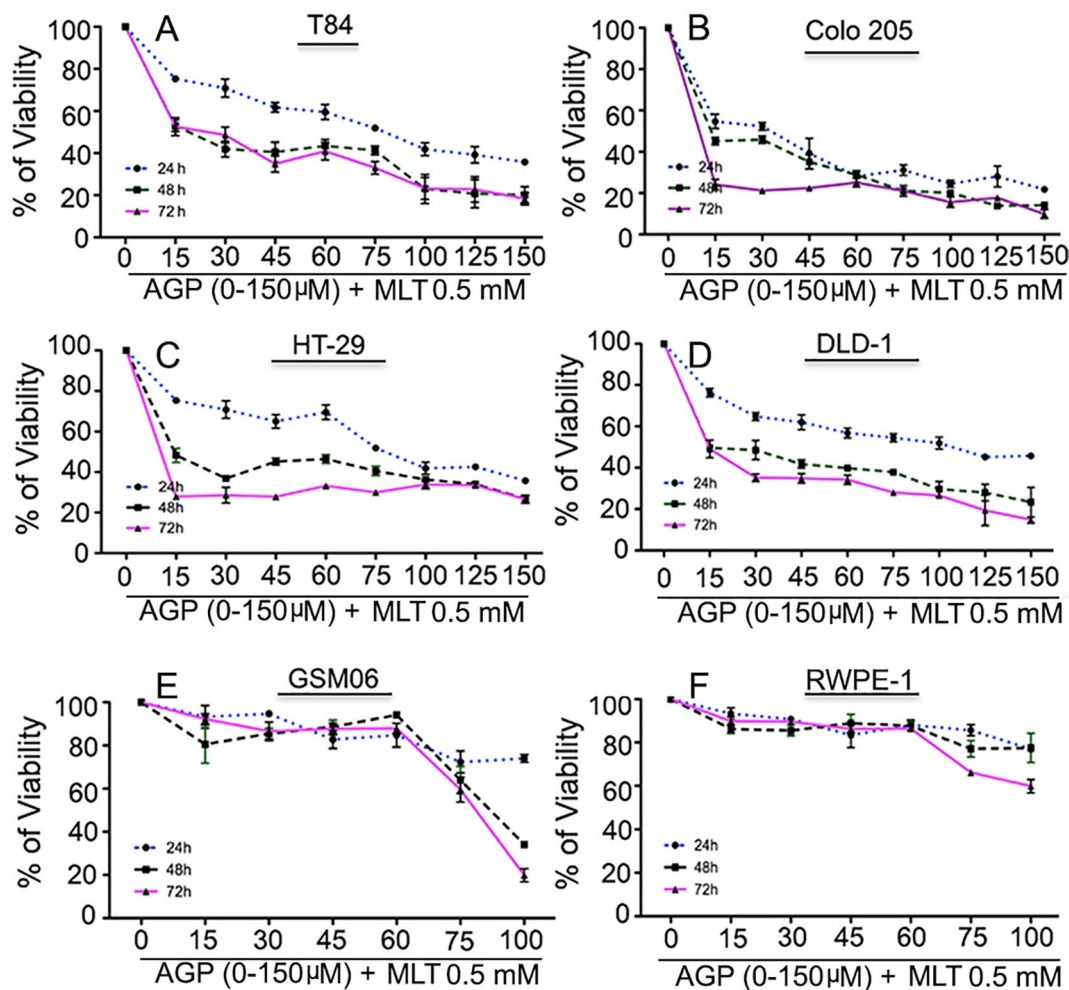


Figure 1. Impact of AGP and MLT on mCRC cell viability: (A) T84, (B) Colo 205, (C) HT-29, (D) DLD-1, (E) GSM06 (gastric surface mice mucous), and (F) RWPE-1 (prostate epithelial cells were treated with indicated concentration of AGP (0-150 μ M), and MLT (0.5 mM) for 24, 48, and 72 hours. Cell viability was quantified using the MTT assay. AGP indicates andrographolide; MLT, melatonin.

and ATF-6 expression in T84 co-treated group (Figure 4E, F, and H). Taken together, the results indicate that co-treatment-induced apoptosis is mediated via ER stress and the IRE-1 activation pathway.

Co-treatment induced G2/M cell cycle arrest and involvement of ROS molecules

AGP alone suppresses Cyclin B1 expression in T84 and Colo 205 cell lysates.⁸ To monitor the Cyclin B1 expression in co-treatment groups, T84 and Colo 205 cells were treated with or without AGP and MLT. The cell lysates were analyzed for Cyclin B1 expression. Figure 5A and A1 show AGP and MLT could effectively suppress Cyclin B1 expression ($P < .001$) as compared with untreated control and AGP or MLT alone groups. Next, we monitored antioxidant protein expression (Prx and Trx) by western blot. Peroxiredoxin (Prx) and Thioredoxin-1 (Trx-1) are upregulated in many human cancers, including colon and rectum,

and in some cancers, downregulation of Prx promotes apoptosis.²⁴⁻²⁶

Our findings indicate co-treatment significantly downregulates Prx and Trx expression (Figure 5B and B1; $P < .05$, $P < .001$) in both cell lysates. Taken together, the results depicted that co-treatment causes cell cycle arrest through downregulation of cyclin B1 and Prx- and Trx-mediated oxidative stress-induced cell apoptosis.

Impact of AGP and MLT on patient-derived organoids

Patient-derived organoids were generated as previously described⁹ (Figure 6A). Matured organoids were treated with or without AGP (15 μ M) and MLT (0.5 mM) for 48 hours. A loss of membrane integrity was found in the co-treatment group as compared with the AGP or MLT alone groups. Untreated group retained the structure of 3D organoids with intact membrane integrity (Figure 6B). Immunofluorescence

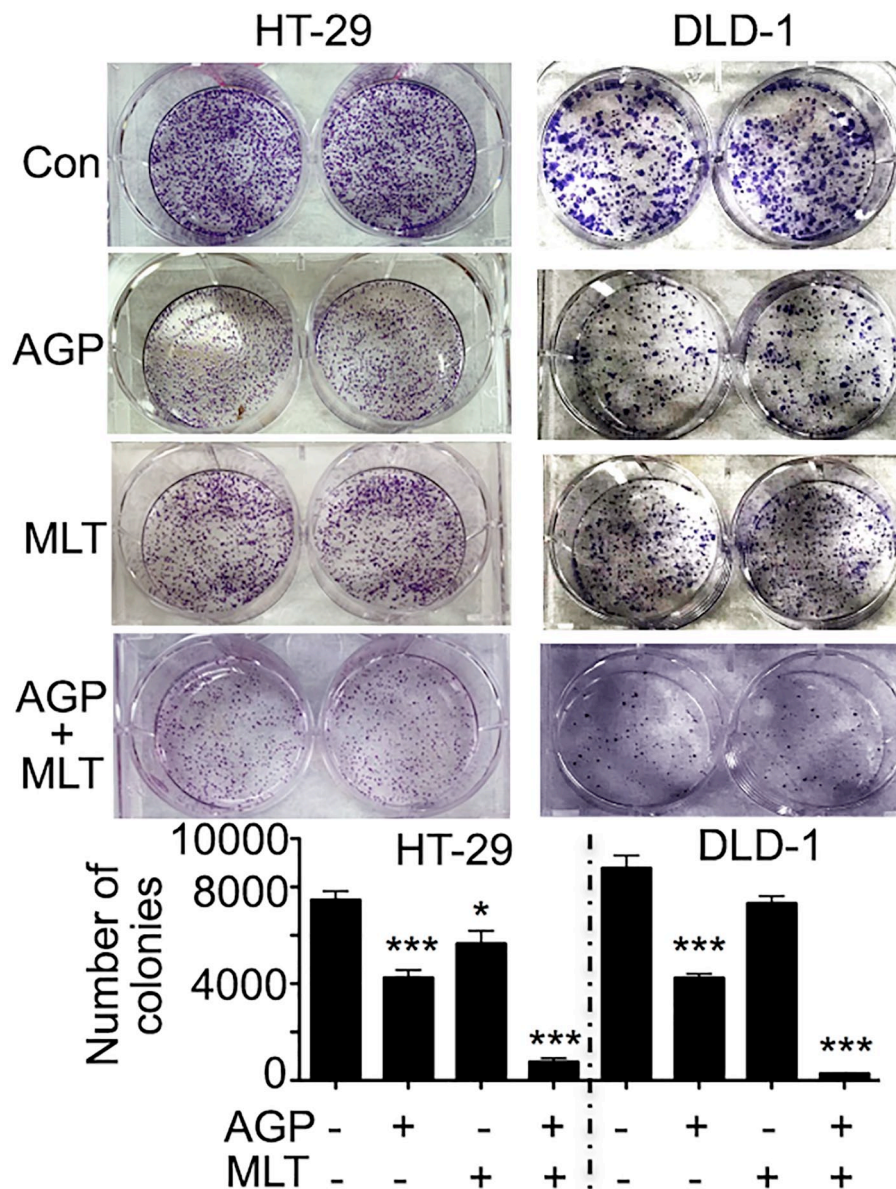


Figure 2. Co-treatment suppresses clonogenicity in HT-29 and DLD-1 cells. HT-29 and DLD-1 cells were diluted and treated with AGP and MLT as indicated dose. Growth was measured by direct counting of clonal clusters stained in multiwell plates with crystal violet at 48 hours. Representative micrographs are shown. AGP indicates andrographolide; MLT, melatonin.

staining for Ki-67 expression was evaluated to measure the effect of AGP, MLT, or co-treatment of AGP and MLT on organoids growth. Ki-67 was greatly reduced in all treatment groups as compared with the untreated group; maximum reduction was found in the co-treatment group (Figure 6C).

Discussion

CRC is the third most prevalent malignant tumor worldwide and the number of new cases may increase to nearly 2.5 million in 2035.^{27,28} The 5-year survival rate for CRC is ~64%, but drops to 12% for metastatic CRC, and therefore, additional treatment regimens are needed to develop effective approaches for medical intervention.²⁹

Previous studies have demonstrated that AGP alone causes inhibition of CRC cell proliferation in metastatic cell lines and patient-derived organoids at a concentration of 45 μ M. The inhibition was shown to be due to ER stress-mediated apoptosis.⁷⁻⁹ Moreover, AGP displayed synergistic effect with chemotherapeutic drugs in CRC cells and hepatocellular carcinoma cells.^{30,31} In vitro and in vivo studies have demonstrated the significant role AGP can have in re-sensitizing 5-Fu-resistant HCT116 (HCT116/5-FuR) cells to the cytotoxic effects of 5-Fu. AGP reverses 5-Fu resistance in human CRC through increasing the expression of BAX.¹¹ AGP, either alone or in combination with cisplatin, also induces CRC apoptotic cell death via increasing the expression of BAX and Bcl-2 and

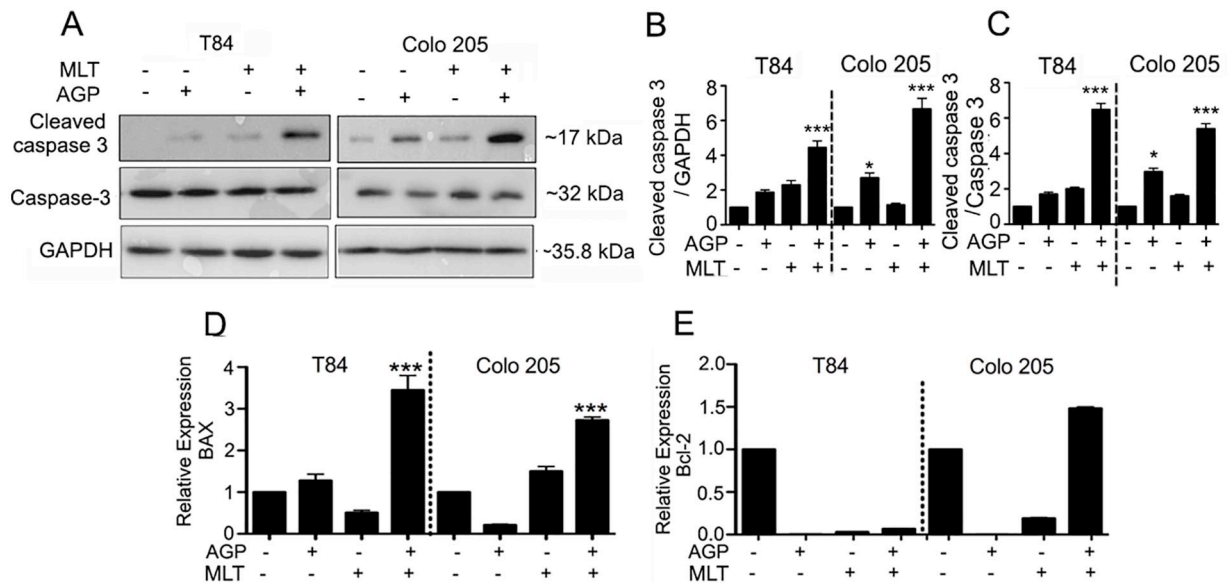


Figure 3. Co-treatment of AGP and MLT-induced cell apoptosis. T84 and Colo 205 cells were treated with or without AGP and MLT at IC_{50} for 48 hours and protein expression was determined by immunoblotting for Cleaved caspase 3 (A, upper lane), Caspase 3 (A, middle lane) and GAPDH (A, lower lane). Densitometry analysis was performed and normalized with GAPDH expression to determine significant upregulation of indicated proteins (B and C). The mRNA level for apoptosis-associated genes was determined by qRT-PCR for BAX (D), Bcl-2 (E). Bar graphs show quantitative results normalized to GAPDH mRNA levels. Results are from 3 independent experiments. Statistical significance was determined using 1-way ANOVA followed by Bonferroni test (* $P < .05$, ** $P < .01$, *** $P < .001$). AGP indicates andrographolide; ANOVA, analysis of variance; GAPDH, glyceraldehyde-3-phosphate dehydrogenase; MLT, melatonin; qRT-PCR, quantitative real-time polymerase chain reaction.

increasing the association of Fas and FasL.³² Additional study provided the evidence for its possible clinical application in enhancing the antitumor effect.³³ Recently, it is reported the synergistic cytotoxicity of AGP and MLT in mCRC cell lines, colospheroids and 5-FU drug resistance cells³⁴ and the molecular mechanism is apoptosis due to UPR-mediated ER stress and angiogenic inhibition. In this study, we have used a combination of AGP and MLT for metastatic CRC cell inhibition as both compounds have antiangiogenic, apoptotic, cell cycle arrest dysregulation of various cancer signaling pathways and involved in regulation of immune function and tumor micro-environments.³⁴ Here, we examined the uses of a lower concentration of AGP when administered in combination with MLT (0.5 mM). The therapeutic concentration of MLT (0.5 mM) was selected because it modulates several signaling pathways which are considered likely antimetastasis, antiproliferative, and pro-apoptotic pathways in cancer cells.^{13,17,23,35,36} Moreover, MLT does not show undesired side effects, even at extremely high doses.^{37,38} However, on pharmacological grounds, MLT can be designated as a synergistic or potentiating effect and it may have a potential clinical implication in the treatment of several pathologies including neurodegenerative diseases.³⁹ In addition, it inhibits CRC stem cells by regulating the PrP^c-Oct4 axis. A synergistic effect has also been observed with MLT when combined with 5-Fu by inhibiting the stem cell markers Oct4, Nanog, Sox2, and ALDH1A1 through regulation of PrP^c.¹⁷

We screened the potential effect of an AGP and MLT co-treatment on a panel of CRC cells and normal cells. The IC_{50} value of AGP in co-treatment is reduced 3-fold compared with AGP alone.^{7,8} Co-treatment of AGP and MLT inhibits cell viability and has significantly less cytotoxicity in mouse normal epithelial cells and human prostate epithelial cells. Co-treatment induces an increase in mRNA and protein levels of IRE-1, 1 of the 3 major ER stress activated UPR proteins; an observation that is consistent between 2 cell lines. Increases in transcription of ATF6 mRNA were observed in T84 and Colo 205 cells, but protein levels only increased in T84 cell lysates at 48 hours. Therefore, involvement of UPR protein at 48 hours is associated with an increase in pro-apoptotic signaling and cell death.

ROS generation can induce carcinogenesis by stimulating mutation and can inhibit tumor progression by inducing apoptotic signals.⁴⁰ Studies have demonstrated the importance of ROS in AGP-induced anticancer cell activities.⁸ Among the Prx family of proteins, Prx-1 is the most prominent subtype with an increase in expression in tumor tissues.⁴¹ Trx-1, a small redox protein, also has shown an increase in expression when observed in many human cancers including colon cancer. We have observed that co-treatment downregulates Prx-1 and Trx expression, which is consistent with the elevated expression of cleaved caspase 3, CHOP, and XBP-1 and the decreased expression of Cyclin B1.

Patient-derived models are necessary to improve knowledge about CRC and to develop new therapeutic approaches. Our

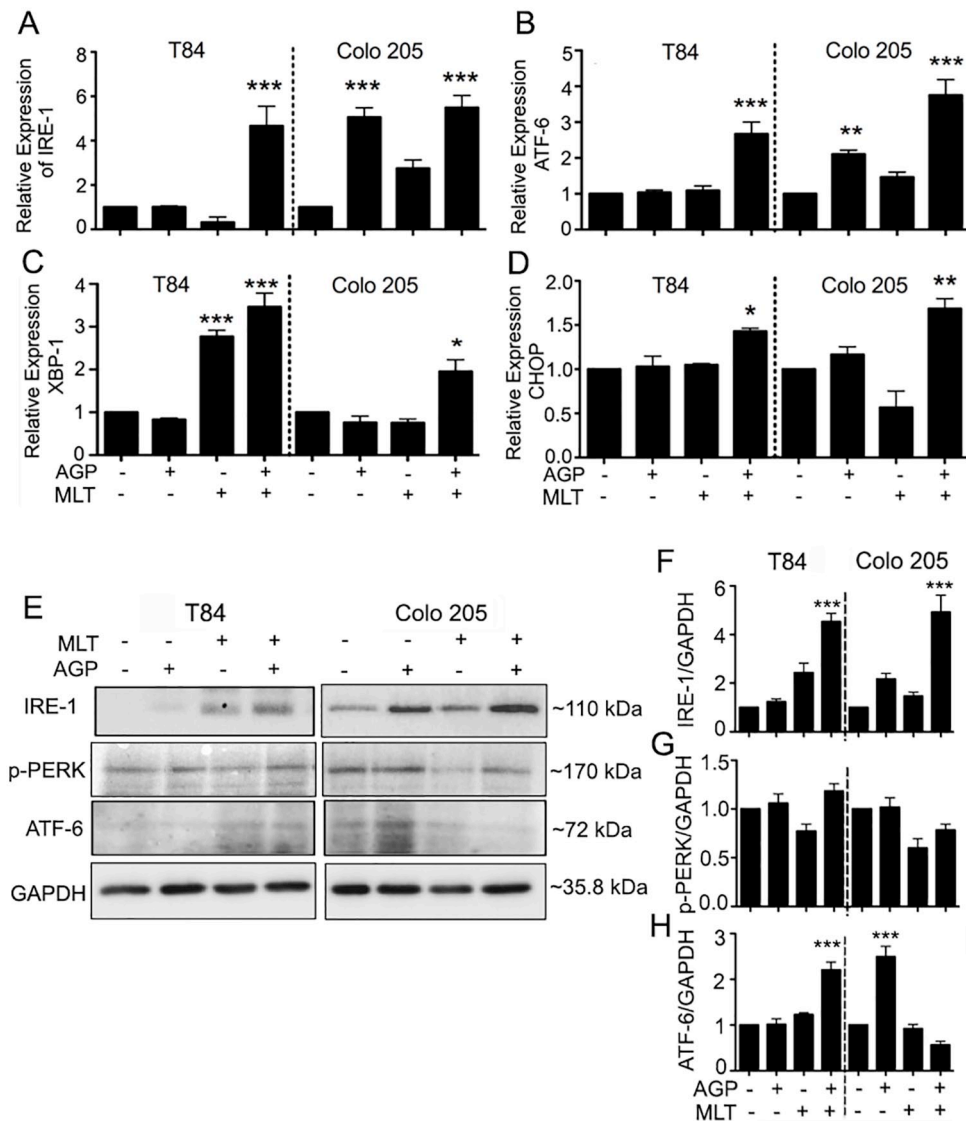


Figure 4. AGP and MLT induces ER stress-related IRE-1 and associated proteins. T84 and Colo 205 cells were treated as mentioned earlier. The transcriptional level of expression for ER stress associated genes was determined by qRT-PCR for (A) IRE-1, (B) ATF-6, (C) XBP-1, and (D) CHOP. Bar graphs show quantitative results normalized to GAPDH mRNA levels. The primary ER transducer translational level was determined by immunoblotting for (E) IRE-1 (level-1), p-PERK (level-2), and ATF-6 (level-3). Densitometry analysis was performed and normalized with GAPDH (blot 4) (F-H). Results are from 3 independent experiments. Statistical significance was determined using 1-way ANOVA followed by Bonferroni test ($*P < .05$, $**P < .01$, $***P < .001$). AGP indicates andrographolide; ANOVA, analysis of variance; ER, endoplasmic reticulum; GAPDH, glyceraldehyde-3-phosphate dehydrogenase; MLT, melatonin; qRT-PCR, quantitative real-time polymerase chain reaction.

model represents an informative system employing both in vitro and ex vivo testing, support by a previous study.⁴² Our data show the impact of AGP and MLT on the inhibition of organoid morphology derived from third metastatic CRC patient tissue, which corroborates the inhibition of Ki67. A significant amount of Ki67 in organoids in the untreated group is consistent with another study which reports elevated Ki67 in CD133⁺, CD44⁺/CD24⁻, and ALDH⁺ CSCs.⁴³ Multiple studies have demonstrated that besides having a role in cell proliferation, Ki67 is also involved in metastasis and invasion of cancer cells.^{43,44} These studies support a role for dual therapy using the natural products AGP and MLT against CRC.

Conclusions

This is the first report analyzing the potential of dual AGP and MLT treatment on CRC using CRC cell lines as well as patient-derived CRC organoids. The dual treatment was demonstrated to inhibit cell viability and promote cell cycle arrest as well as promote ER stress-dependent apoptosis signaling in CRC cell lines. Cancer organoids derived from metastatic CRC were also shown to display membrane disruption and reduced proliferative activity in response to AGP and MLT treatment compared with control organoids. The molecular mechanisms that contribute to cell death in CRC cells in response to AGP and MLT remain unclear. Therefore, further

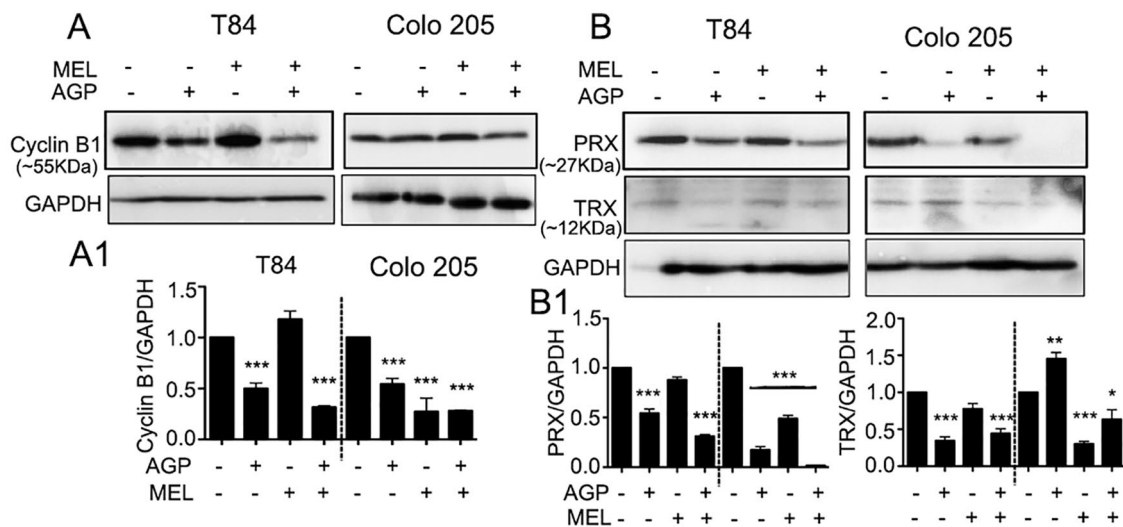


Figure 5. Co-treatment induced cell cycle arrest and decreased antioxidant protein expression in CRC cells. T84 and Colo 205 cells were treated with or without AGP (15 μ M) and MEL (0.5mM) for 48 hours. Cell lysates were analyzed by immunoblot for cyclin B1 (A), PRX (B, upper lane), and TRX (B, middle lane) and quantified by densitometry for expression of (A1) Cyclin B1, (B1) (left) PRX and (right) TRX. Expression is normalized against GAPDH expression. Statistical significance was determined using 1-way ANOVA followed by Bonferroni test (* $P < .05$, ** $P < .01$, *** $P < .001$). AGP indicates andrographolide; ANOVA, analysis of variance; CRC, colorectal cancer; GAPDH, glyceraldehyde-3-phosphate dehydrogenase.

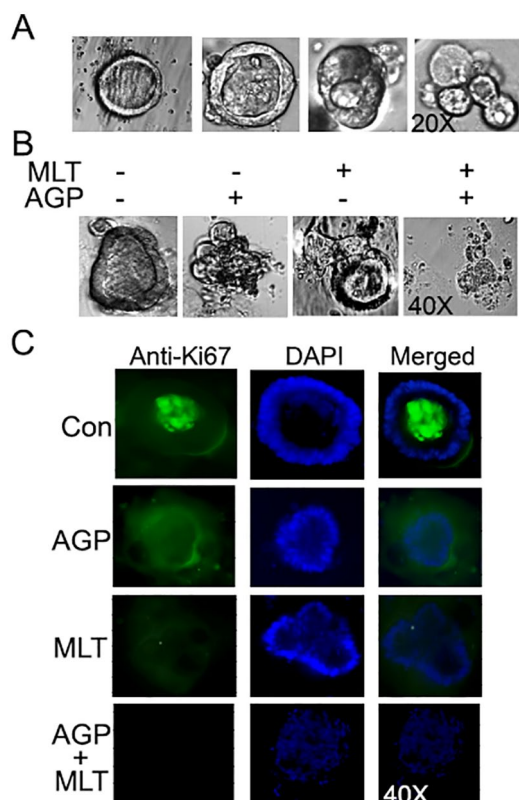


Figure 6. Impact of AGP and MEL on patient-derived organoids (PDOD). (A) Chronological development of PDOD in Matrigel droplet. Organoid structures were confirmed using an inverted light microscope. (B) PDOD were treated with or without AGP or MEL and morphology was assessed by light microscopy. (C) FITC labeled anti-Ki-67 and DAPI staining of PDOD in the presence or absence of AGP or MEL evaluated by fluorescence microscopy. AGP indicates andrographolide; MELT, melatonin; PDOD, patient-derived organoids.

investigation on this combination therapy will be necessary to delineate the molecular interactions within the CRC PDOD model.

Author Contributions

T.G.B., S.J.C., and Ad.B. contributed to conceptualization. An.B. provided the surgical tissues. N.S., T.I., E.H., and S.G. performed the experiments and analyzed the data. N.S. and Ad.B. contributed to writing the original draft. T.G.B., S.J.C., and Ad.B. contributed to reviewing and editing. Ad.B. supervised the study. All authors have read and approved the final manuscript.

Availability of Data and Materials

The datasets generated and analyzed during the current study are not publicly available due to continuing the research but are available from the corresponding author on reasonable request.

Ethics Approval and Consent to Participate

University of Maryland Institutional Review Board (HP-00066889-3).

ORCID iD

Aditi Banerjee <https://orcid.org/0000-0003-1608-2998>

Supplemental Material

Supplemental material for this article is available online.

REFERENCES

1. American Cancer Society. Survival rates for colorectal cancer. <https://www.cancer.org/cancer/colon-rectal-cancer/detection-diagnosis-staging/survival-rates.html>. Published 2020.

2. Chapuis PH, Bokey E, Chan C, et al. Recurrence and cancer-specific death after adjuvant chemotherapy for Stage III colon cancer. *Colorectal Dis.* 2019; 21:164-173.
3. Dienstmann R, Salazar R, Tabernero J. Personalizing colon cancer adjuvant therapy: selecting optimal treatments for individual patients. *J Clin Oncol.* 2015;33:1787-1796.
4. Hodgkinson N, Kruger CA, Abrahamse H. Targeted photodynamic therapy as potential treatment modality for the eradication of colon cancer and colon cancer stem cells. *Tumour Biol.* 2017;39:1010428317734691.
5. Bayat Mokhtari R, Homayouni TS, Baluch N, et al. Combination therapy in combating cancer. *Oncotarget.* 2017;8:38022-38043.
6. Wang Z, Wei Y, Fang G, et al. Colorectal cancer combination therapy using drug and gene co-delivered, targeted poly(ethylene glycol)-epsilon-poly(caprolactone) nanocarriers. *Drug Des Devel Ther.* 2018;12:3171-3180.
7. Banerjee A, Ahmed H, Yang P, Czinn SJ, Blanchard TG. Endoplasmic reticulum stress and IRE-1 signaling cause apoptosis in colon cancer cells in response to andrographolide treatment. *Oncotarget.* 2016;7:41432-41444.
8. Banerjee A, Banerjee V, Czinn S, Blanchard T. Increased reactive oxygen species levels cause ER stress and cytotoxicity in andrographolide treated colon cancer cells. *Oncotarget.* 2017;8:26142-26153.
9. Blanchard TG, Lapidus R, Banerjee V, et al. Upregulation of RASSF1A in colon cancer by suppression of angiogenesis signaling and Akt activation. *Cell Physiol Biochem.* 2018;48:1259-1273.
10. Islam MT, Ali ES, Uddin SJ, et al. Andrographolide, a diterpene lactone from *Andrographis paniculata* and its therapeutic promises in cancer. *Cancer Lett.* 2018;420:129-145.
11. Wang W, Guo W, Li L, et al. Andrographolide reversed 5-FU resistance in human colorectal cancer by elevating BAX expression. *Biochem Pharmacol.* 2016;121:8-17.
12. Akbarzadeh M, Movassaghpour AA, Ghanbari H, et al. The potential therapeutic effect of melatonin on human ovarian cancer by inhibition of invasion and migration of cancer stem cells. *Sci Rep.* 2017;7:17062.
13. Hao J, Fan W, Li Y, et al. Melatonin synergizes BRAF-targeting agent vemurafenib in melanoma treatment by inhibiting iNOS/hTERT signaling and cancer-stem cell traits. *J Exp Clin Cancer Res.* 2019;38:48.
14. Su SC, Hsieh MJ, Yang WE, Chung WH, Reiter RJ, Yang SF. Cancer metastasis: mechanisms of inhibition by melatonin. *J Pineal Res.* 2017;62:e12370.
15. Gil-Martin E, Egea J, Reiter RJ, Romero A. The emergence of melatonin in oncology: focus on colorectal cancer. *Med Res Rev.* 2019;39:2239-2285.
16. Buldak RJ, Pilc-Gumula K, Buldak L, et al. Effects of ghrelin, leptin and melatonin on the levels of reactive oxygen species, antioxidant enzyme activity and viability of the HCT 116 human colorectal carcinoma cell line. *Mol Med Rep.* 2015;12:2275-2282.
17. Lee JH, Yun CW, Han YS, et al. Melatonin and 5-fluorouracil co-suppress colon cancer stem cells by regulating cellular prion protein-Oct4 axis. *J Pineal Res.* 2018;65:e12519.
18. Banerjee A. Organoid culture and its importance. *Gastroenterol Hepatol Int J.* 2017;2:1-2.
19. Blanchard TG, Czinn SJ, Banerjee V, et al. Identification of cross talk between FoxM1 and RASSF1A as a therapeutic target of colon cancer. *Cancers (Basel).* 2019;11:199.
20. Banerjee A, Basu M, Blanchard TG, et al. Early molecular events in murine gastric epithelial cells mediated by *Helicobacter pylori* CagA. *Helicobacter.* 2016;21:395-404.
21. Wiener Z, Band AM, Kallio P, et al. Oncogenic mutations in intestinal adenomas regulate Bim-mediated apoptosis induced by TGF-beta. *Proc Natl Acad Sci USA.* 2014;111:E2229-E2236.
22. Garcia-Navarro A, Gonzalez-Puga C, Escames G, et al. Cellular mechanisms involved in the melatonin inhibition of HT-29 human colon cancer cell proliferation in culture. *J Pineal Res.* 2007;43:195-205.
23. Liu Z, Zou D, Yang X, et al. Melatonin inhibits colon cancer RKO cell migration by downregulating Rho associated protein kinase expression via the p38/MAPK signaling pathway. *Mol Med Rep.* 2017;16:9383-9392.
24. Kim H, Lee GR, Kim J, et al. Sulfiredoxin inhibitor induces preferential death of cancer cells through reactive oxygen species-mediated mitochondrial damage. *Free Radic Biol Med.* 2016;91:264-274.
25. Lin F, Zhang P, Zuo Z, et al. Thioredoxin-1 promotes colorectal cancer invasion and metastasis through crosstalk with S100P. *Cancer Lett.* 2017;401:1-10.
26. Raffel J, Bhattacharyya AK, Gallegos A, et al. Increased expression of thioredoxin-1 in human colorectal cancer is associated with decreased patient survival. *J Lab Clin Med.* 2003;142:46-51.
27. Dekker E, Tanis PJ, Vleugels JLA, Kasi PM, Wallace MB. Colorectal cancer. *Lancet.* 2019;394:1467-1480.
28. Xie YH, Chen YX, Fang JY. Comprehensive review of targeted therapy for colorectal cancer. *Signal Transduct Target Ther.* 2020;5:22.
29. Siegel RL, Miller KD, Jemal A. Cancer statistics, 2019. *CA Cancer J Clin.* 2019;69:7-34.
30. Khan I, Mahfooz S, Ansari IA. Antiproliferative and apoptotic properties of andrographolide against human colon cancer DLD1 cell line. *Endocr Metab Immune Disord Drug Targets.* 2020;20:930-942.
31. Yang L, Wu D, Luo K, Wu S, Wu P. Andrographolide enhances 5-fluorouracil-induced apoptosis via caspase-8-dependent mitochondrial pathway involving p53 participation in hepatocellular carcinoma (SMMC-7721) cells. *Cancer Lett.* 2009;276:180-188.
32. Lin HH, Shi MD, Tseng HC, Chen JH. Andrographolide sensitizes the cytotoxicity of human colorectal carcinoma cells toward cisplatin via enhancing apoptosis pathways in vitro and in vivo. *Toxicol Sci.* 2014;139:108-120.
33. Su M, Qin B, Liu F, Chen Y, Zhang R. Andrographolide enhanced 5-fluorouracil-induced antitumor effect in colorectal cancer via inhibition of c-MET pathway. *Drug Des Devel Ther.* 2017;11:3333-3341.
34. Banerjee V, Sharda N, Huse J, et al. Synergistic potential of dual andrographolide and melatonin targeting of metastatic colon cancer cells: using the Chou-Talalay combination index method. *Eur J Pharmacol.* 2021;897:173919.
35. Reiter RJ, Rosales-Corral SA, Tan DX, et al. Melatonin, a full service anti-cancer agent: inhibition of initiation, progression and metastasis. *Int J Mol Sci.* 2017;18:843.
36. Reiter RJ, Sharma R, Ma Q, Rosales-Corral S, de Almeida Chuffa LG. Melatonin inhibits Warburg-dependent cancer by redirecting glucose oxidation to the mitochondria: a mechanistic hypothesis. *Cell Mol Life Sci.* 2020;77:2527-2542.
37. Banerjee A, Czinn SJ, Reiter RJ, Blanchard TG. Crosstalk between endoplasmic reticulum stress and anti-viral activities: a novel therapeutic target for COVID-19. *Life Sci.* 2020;255:117842.
38. Fic M, Gomulkiewicz A, Grzegorzolka J, et al. The impact of melatonin on colon cancer cells' resistance to doxorubicin in an in vitro study. *Int J Mol Sci.* 2017;18:1396.
39. Romero A, Egea J, Garcia AG, Lopez MG. Synergistic neuroprotective effect of combined low concentrations of galantamine and melatonin against oxidative stress in SH-SY5Y neuroblastoma cells. *J Pineal Res.* 2010;49:141-148.
40. Majumder DNP, Debnath R, Maiti D. Understanding the complicated relationship between antioxidants and carcinogenesis. *J Biochem Mol Toxicol.* 2021;35:e22643.
41. Kim YJ, Ahn JY, Liang P, Ip C, Zhang Y, Park YM. Human prx1 gene is a target of Nrf2 and is up-regulated by hypoxia/reoxygenation: implication to tumor biology. *Cancer Res.* 2007;67:546-554.
42. Grassi L, Alfonsi R, Francescangeli F, et al. Organoids as a new model for improving regenerative medicine and cancer personalized therapy in renal diseases. *Cell Death Dis.* 2019;10:201.
43. Li FY, Wu SG, Zhou J, et al. Prognostic value of Ki-67 in breast cancer patients with positive axillary lymph nodes: a retrospective cohort study. *PLoS ONE.* 2014;9:e87264.
44. Cidado J, Wong HY, Rosen DM, et al. Ki-67 is required for maintenance of cancer stem cells but not cell proliferation. *Oncotarget.* 2016;7:6281-6293.